International Journal of Thermofluids 27 (2025) 101189

Contents lists available at ScienceDirect

International Journal of Thermofluids

journal homepage: www.sciencedirect.com/journal/international-journal-of-thermofluids

Enhancing energy efficiency in buildings using phase-change materials, acrylic paint, and solar shading in hot climates

Mohammed ALamin Talib Mahdi [a,*], Mousa Nader [b,g], Humam Yagdan [c], Sajjad Tariq [d], Amar S. Abdul-Zahra [a], Hussaen A.H. Kahachi [e,f]

[a] Department of Mechanical Engineering, University of Technology-Iraq, Baghdad, Iraq
[b] Department of Mechanical Engineering, University of Debrecen, Debrecen, Hungary
[c] Department of Chemical Engineering, University of Technology-Iraq, Baghdad, Iraq
[d] Department of Electromechanical Engineering, University of Technology-Iraq, Baghdad, Iraq
[e] Department of Architectural Engineering, University of Technology, Baghdad, Iraq
[f] Department of Land Economy, University of Cambridge, Cambridge, United Kingdom
[g] University Of Technology-Iraq, Baghdad, Iraq

ARTICLE INFO

Keywords:
PCM
Sustainable building
Thermal insulation
Building's shading
CFD

ABSTRACT

In 2023, total greenhouse gas (GHG) emissions around the globe increased to 41.6 billion metric tons of CO_2 equivalent. Most of this emissions increase came from the use of residential electricity. In this regard, this study introduces a new integrated approach to enhancing energy-efficient buildings. This is in the above-mentioned context as it explores promising passive cooling strategies for reducing energy consumption and emissions in hot climatic conditions of the Middle East regions. The analysis incorporates integrating phase-change material (PCMs) with the reflective coating and the shading by solar PV panels not fully considered in other studies. In contrast to the conventional usage of PCMs or reflective coatings alone, it is found that their combination provides for a far better thermal management system for the building for minimizing heat absorption while allowing greater heat redistribution. Using ANSYS FLUENT software, experiments of the designs, the cooling loads, and CO_2 emissions were validated through experiments conducted in earlier studies. The investigation shows that defining PCM integration and reflective coating individually reduces heat gain by 76.57 %,56.70 %, respectively; however, due to the greater microclimate efficiency of the building, these configurations do not yield the greatest heat gain reduction. Using PV panels as roof shaders show a 92.69 % heat gain reduction, and combining the reflective coating with PCM integration produced an 84.12 % reduction. Thus, it was found that the mass of CO_2 emissions was 5.767 kg, 3.797 kg, 0.671 kg, and 2.114 kg for the respective 4 days for the cases of reflective coating, PCM integration, PV-shading and of reflective coating and PCM combined, respectively. This gives a direct comparison of several roof systems under hot climates for the first time and will aid in sustainable building design and climate resilience engineering.

1. Introduction

Global greenhouse gas emissions totaled 41.6 billion metric tons of CO_2 equivalent, a 2 % increase from 2024 [1]. Electricity generation, a key aspect of human development, continues to be the primary engine of climate change [2]. The annual global electricity consumption per person was predicted to be 21,394 kW-hours in 2023, being among the main sources. In contrast, the average amount of electricity per person is 19,239 kWh in Asian states. This explicitly shows that the discrepancy in consuming electricity is the leading cause that divides these regions apart [3]. However, the report says this increased in homes primarily, and thus, It is now critical to take decisive steps to reduce electricity needs, thereby lowering both those demands and greenhouse gas emissions, through rapid adoption of sustainable solutions [4]. Nowadays one of the most concerning things is that the pollution in the Eastern Mediterranean and the Middle East has exacerbated greenhouse gas emissions (GHGs) causing the environment to be affected adversely. This particular direction, without any doubt, signifies a definite and immediate directive to implement actions that can be genuinely revolutionary for the region towards ending the climate change crisis [5]. Moreover, A report by the U.S. Energy Information Administration (EIA)

* Corresponding author at: Department of Mechanical Engineering, University of Technology-Iraq.
E-mail address: mohammed.a.talib@uotechnology.edu.iq (M.A.T. Mahdi).

https://doi.org/10.1016/j.ijft.2025.101189

Available online 30 March 2025

Nomenclature

A	The surface area perpendicular to the layer
C_p	Heat capacity
e	Internal energy
ΔE	Total energy saved
h	Enthalpy
h_f	Melting heat of fusion
h_j	Enthalpy of species j.
$\vec{J_j}$	The diffusion flux of species j.
k	Thermal conductivity
k_{eff}	The effective thermal conductivity
m	Mass of PCM
m_α	Mass of melted PCM
p	Pressure
q	Heat flow
q_l	Latent thermal energy stored
q_s	Sensible thermal energy stored
R_{th}	Thermal resistance
S_h	Volumetric heat sources
T	Temperature
T_l	PCM liquid state temperature
T_0	Reference temperature of air
T_s	PCM solid-state temperature
t	Time
V	Velocity vector of air
X	Layer thickness

Greek symbols

α	Liquid fraction
β	Thermal expansion coefficient
μ	Dynamic viscosity of air
ρ	Density
ρ_l	PCM liquid state density
ρ_0	Reference density of air
ρ_s	PCM solid-state density
τ_{eff}	Effective stress tensor
Ψ	Co2 mass

declares that 35 % of the electrical consumption needed in some areas is consumed by residential buildings [6]. Addressing this sector could play a pivotal role in improving energy efficiency in residential buildings, which can significantly reduce overall emissions [7]. According to J. Torres et al. [8], roof insulation is extremely important because 56 % of the gain of a building's solar heat is attributed to the roof. The absence of a good insulating material leaves behind surplus heat, thus calling for extra air conditioning, which in turn causes more electricity to be used. New studies have supported that thermal insulation is instrumental in the energy efficiency of buildings [9–11], thus contributing to the decrease of GHG emissions. Scientific experiments have proven that innovative thermal insulating methods, such as polyurethane wall insulation, can reduce the cooling loads by 73 % [12]. A. Husseinet. al demonstrates that a 5 cm layer of natural stone on the wall layer acts as an insulator and can minimize thermal leakage by 49 % when the window-to-wall ratio is under 25 % [13]. These findings demonstrate the promise of insulation improvements in the reduction of energy consumption. In conjunction with traditional offerings, environmentally viable options like the use of chemical-treated wooden insulators have come to light. These materials are reported to have a thermal conductivity of 0.038 W/(m·K) which is 5 % less than that of the expanded polystyrene type and has become more efficient [14]. Furthermore, Mahmood et.al. utilized an innovative and very effective technique by using locally made insulation material such as reed mat, sawdust, and cork grains as a two-layered insulated wall treated chemically. In particular, the excitation of these sawdust mats by only energy combines 50 % of not using the sun and this makes them also environmentally friendly. 44 % of the sawdust used for production and 40 % of the cork grains used in the process also present the same positive effect [15]. Phase-change materials (PCMs) have emerged as another innovative solution. By the process of storing and releasing heat in phase transition, PCM enhances indoor temperature stabilization and consequently leads to lower cooling needs. Integrating PCM with walls, floors, and ceilings has been found to be an important method to reduce CO_2 emissions, even reaching up to 76.57 % in some cases [16–22]. Additionally, using a 2 cm air gap, with PCM insulation could result in a decrease of about 72–75 % heat gain and a reduction of meteorological variability by 4–7 °C [23]. Though the problem of less heat loss during the night with more PCM layers is faced, it is difficult to eliminate this drawback. To address this, PCM insulation and roof ventilation, both when employed together, can solve the problem of not good heat dissipation at night. CFD analysis displays settings that are projected to work best, for example, a melting point of 35–37 °C with ventilation speeds of 2.4 m/s can lower the maximum temperature by 4.11 °C [24]. Also, PCMs as a layer integrated inside walls or roofs is not the only form that can be used. For example, using cylindrical aluminum capsules containing PCM in the outer row of bricks reduced the room temperature by 1.9 °C, while placement in the inner row reduced the temperature by 2.7 °C [25]. Another form of PCM in building envelops is capsules, combining them with a metal sheet roof results inner room temperature reduction [26]. after 4 types of PCM testing, they concluded that the highest melting point (59 °C) PCM had the highest decrease in the inner room temperature compared with other PCMs with lower melting points. However, the selection of the PCM melting temperature is highly dependent on the PCM's position in the room i.e., the medium temperature of the PCM. A recent study examined various parameters impact on heat loss between floors in apartment buildings including different types of PCMs void former shapes, void former placement, and combinations of PCMs and insulating layers [27], over 48 hour time period, a heat flux reduction of 36.74 % was achieved using CT24W PCM type-integrated void formers. Other methods of insulation that can be used include shading the building to prevent solar radiation from reaching the roof. Shading strategies stabilize the insulation methods. For example, during the summer period, shading and adding photovoltaics (IES-VE) to a roof would have the effect of reducing the heat gain by 10.87 %, while the winter heat loss might increase slightly by 3.8 % [28]. In Saudi Arabia, full roof shading has revealed a 12.3 % reduction in cooling loads [29]. The systems that act as a dual purpose, such as Solar PV panels, as shading devices and energy generators, will increase thermal performance and energy efficiency, and thus, renewable integrated energy systems will be the result [30]. Yang Cai studied the potential of the combination of PCM and PV panels on building energy efficiency using TRNSYS software [31], integrating PCM and PV panels in building walls. their exergy analysis shows 11.66 % electrical efficiency enhancement and 1.54 % regarding thermal exergy efficiency, however integrating PCM and PV panels with the roof could have more potential electrically and thermally, which is investigated in the present study, using ANSYS software which is considered as the premier tool for this type of work [32]. The uniqueness of the study concerns integrated passive cooling mechanisms through PCMs, reflective coatings, and sun-shading technologies using PV-panels to improve energy efficiency in any hot region. Unlike previous findings that considered using such techniques in isolation, this study investigates their interaction using ANSYS Fluent 2024 R1, simulating a full-scale room with detailed roof layers for four continuous days, highlighting the PCM melting and solidification process during day and nighttime. The importance of research is further scaled with experimental

validation and thus closes the gap between the simulated and real-world problems. It is indeed a novel study in building thermal sustainability.

2. Methodology

2.1. Geometry design

Five cases were compared for methods of reducing indoor room temperature. In Case A, a basic room without insulation served as the reference. In Case B, the outer surface of the roof is shaded using solar PV panels, for Case C, acrylic paint coating is applied on the outer roof surface. Case D, meanwhile, has incorporated a 3 cm thick PCM layer within the roof structure. Finally, Case E is a combination of Case C acrylic paint and Case D PCM layer. Table 1 summarizes the configurations.

PCM denotes a thermal energy storage material that stores energy through latent heat. It absorbs heat from the environment while keeping a constant temperature during the charging phase. After that, additional heat raises its temperature as sensible heat when it has been completely liquefied. In contrast, at the time of discharging, when the environmental temperature drops below its melting point, the PCM solidifies and releases its stored heat as shown in Fig. 1.

The room sample for this study is a square structure with a floor area of 9 m^2 and a height of 2.8 m, featuring a glass window 1.5 × 1.9 m. The roof consists of many stratifications, representative of traditional Iraqi roofing: concrete tiles, sand, ferroconcrete, and gypsum. These configurations apply to all of the cases, as shown in Fig. 2.

In cases (A), (B), and (C) the roof layers consist of, concrete tiles, sand, ferroconcrete, and gypsum, which is the Iraqi traditional roof configuration. Table 2 summarizes all the material properties being used

2.2. 1-Dimensional (1-D) circuit analogy

This study presents a one-dimensional (1-D) circuit analogy of heat transfer within a room, which can be modeled effectively using Fourier's law of heat conduction. As such, it facilitates the computation of heat penetration through different roof layers, by treating each layer as a plane wall. Thus, heat flow from the outside to the inside of the room can be expressed as the relationship between the overall thermal potential difference to the total thermal resistances of all layers. It is similar to Ohm's law and forms the basis for calculations regarding heat transfer as mathematically depicted in Eqs. (1) to (4) [34]:

$$q = \frac{\Delta T_{overall}}{\sum R_{th}} \tag{1}$$

Here, q is the flow of heat, $\Delta T_{overall}$is the overall temperature difference through the layers, and $\sum R_{th}$ is the total thermal resistance. Thus, in Case A, we derive the equation for heat flow through a room in a 1-D type form:

$$q = \frac{T_2 - T_7}{\sum R_{th}} \tag{2}$$

where: T_2 is the indoor temperature, T_7 is the outdoor temperature.

Additionally, the total thermal resistance is expressed as:

$$\sum_{i}^{n} R_{th} = R_i + \ldots + R_n \;\; \mathrm{i} = \; 1,\; 2,\; 3,\; \ldots,\; \text{etc.} \tag{3}$$

Each thermal resistance R_i is defined as:

$$R_i = \frac{\Delta X_i}{k_i . A} \tag{4}$$

Where ΔX_i is the thickness of the layer *i*, k_i is the thermal conductivity of the layer *i*, A and is the cross-sectional area. Thus, All the thermal resistances from R_2 to R_6 follow a similar format as Eq. (4) but with their specific values for thickness and conductivity as shown in Fig. 3

As previously mentioned phase change materials (PCMs) store heat, both sensibly and latently, and thus, for this, some more calculations need to be done on sensible and latent heat storage. For sensible heat storage q_s, and latent heat storage q_l, the formulations used are(5) to (7) [35]:

$$q_s \;=\; m.\; C_p.\; \Delta T \tag{5}$$

For latent heat storage q_l, we apply:

$$q_l \;=\; m_\alpha . h_f \tag{6}$$

Where, m, m_α is the total mass and melted portion mass of the PCM respectively, $C_p$is the specific heat capacity, ΔT is the temperature change, and h_f. is the latent heat of fusion. Noting that the m_α can be described as:

$$m_\alpha \;=\; m \;.\; \alpha, where\; \alpha\; is the melt fraction \tag{7}$$

Finally, to quantify energy savings from implementing enhancement strategies, we compare energy consumption between basic and enhanced rooms. The energy saved can be expressed as [36]:

$$\Delta E = E_{basic} - E_{enhanced} \tag{8}$$

Where, $E_{basic}$is The energy consumed for the basic room, and $E_{enhanced}$is the energy consumed for the enhanced room.

Fig. 4 shows Iraq's latest data for 2023, where CO_2 emissions come out to be approximately 0.689 $kgCo_2$ / kWh across all other countries. This can lead us to give the formulation for CO_2 emissions for all cases:

$$\Psi \;=\; Co2\; kg/kWh \;\times\; E_{enhanced} \tag{9}$$

Table 1
Simulated cases.

Case	Description
A	Basic room with no enhancements
B	Shaded roof
C	Painted roof
D	PCM layer added roof
E	PCM layer added roof combined with painted roof

2.3. CFD analysis

2.3.1. Simulation assumptions

The CFD analysis in this study was carried out using ANSYS 2024 R1 software. In any simulation case, an appropriate assumptions should be made in the pre-processing stage of the simulation, to direct the study toward a more efficient and clear solution, thus, the following assumptions were made in the present study:

1. The 4 walls and the floor of the room were considered insulated to study the effect of the heat gained from the roof only.

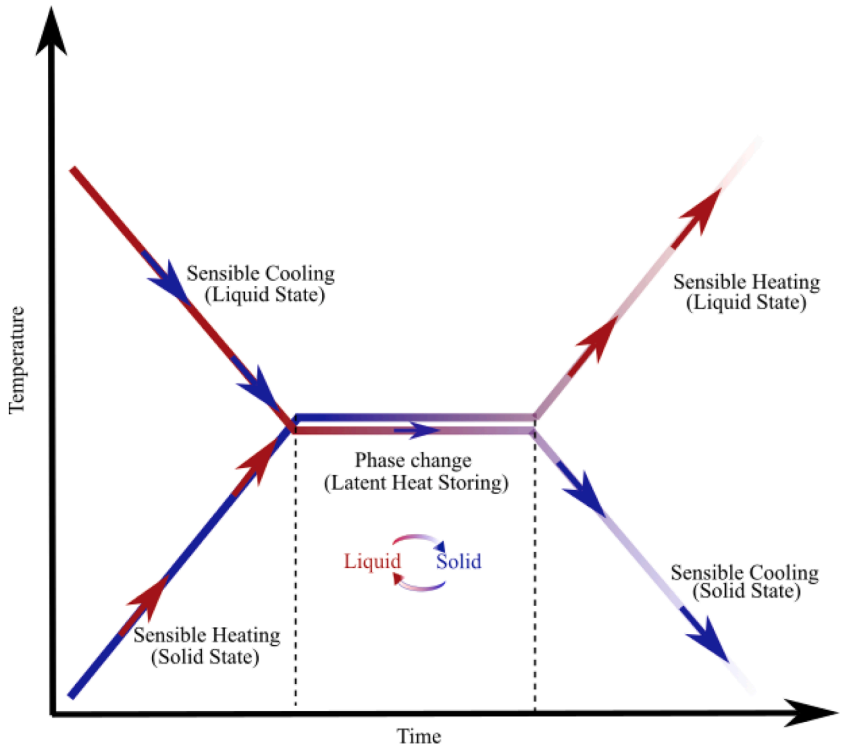

Fig. 1. PCM charging and discharging processes.

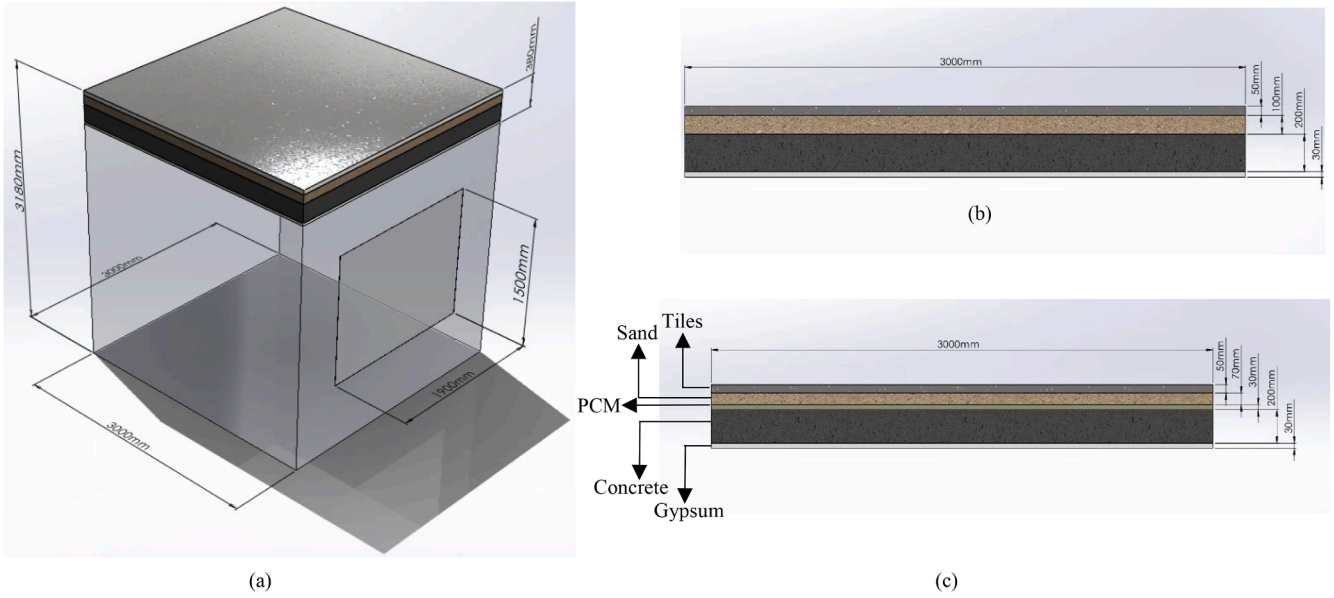

Fig. 2. Room Roof Layers Configuration: (a) Basic room with no type of insulation (b) Roof layers (c) Roof layers with PCM layer(c) Roof layers with PCM layer.

Table 2
Roof layers materials properties [33].

Material	ρ (kg/m^3)	K (w/m.k)	C_p (j/kg.k)
Cement Tiles	2100	1.1	837
Sand	1520	0.33	837
Ferro Concrete	1200	0.38	1000
Gypsum	1200	0.42	837
Glass	2720	0.7	880

2. Meteonorm weather database was used as variable solar radiation and ambient temperature throughout 4 continuous days (from 16 August to 19 August).
3. For simplification, a constant value of convection heat transfer coefficient of 22.7 w/m^2 [33]between the roof surface, room window, and the ambient, neglecting the ambient wind velocity.
4. Convection and conduction heat transfer are only considered through the room's glass window.
5. The solar irradiance is assumed to be generated inside the concrete tiles to make the selection of the convection with the ambient boundary condition in the software possible. Converting heat flux to

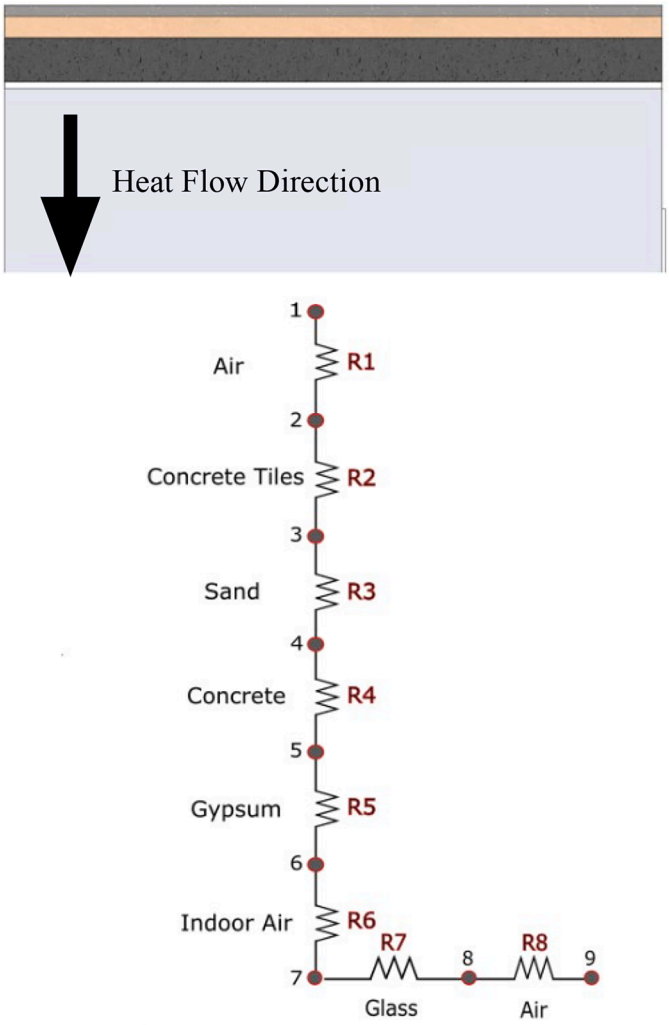

Fig. 3. Room Circuit Analogy.

heat generations by dividing heat flux values by cement tiles thickness.

6. No indoor heat sources.
7. No ventilation is taking place.
8. in case (B), the roof is considered to be fully shaded due to the use of an east-west solar panels configuration that covers the entire roof as shown in Fig. 5. 8 solar panels with 580 w of power are used to cover the area of 9 m^2, facing the east direction, and neglecting the back PV panel radiation and other surfaces effects on the roof.
9. the thermal resistance of the acrylic paint is neglected due to its very thin coating (only the absorption coefficient property is considered).

A grid independence test (GIT) was made to ensure that the simulation results are independent of grid cells. Table 3 shows the GIT made in this study.

The mesh case 4 was chosen through all the simulation cases, as it provides the balance between good accuracy and computation time efficiency, with a maximum skewness value of 0.000827, which means how much the grid cells deviate from its ideal shape, with max aspect ratio of 15.011, aspect ratio is the ratio of the long side of the mesh cell to the shortest side, lower aspect ratio indicating better mesh quality and an orthogonal quality of 1 which is a measure of the deviation of cell faces from being perpendicular, closer to 1 value indicates a high mesh quality, Fig. 6. shows the grid being used. This grid was solved using ANSYS Fluent package through the transient approach.

2.3.2. The governing equations and boundary conditions

Multiple mathematical models were used in this study, like energy, viscous, and melting solidification (in the cases of incorporating the PCM layer in the roof).

For the energy model, the equation used is as follows [38]:

$$\frac{\partial}{\partial t}\left(\rho\left(e+\frac{V^2}{2}\right)\right)+\nabla.\left(\rho V\left(h+\frac{V^2}{2}\right)\right) = \nabla.\left(k_{eff}\nabla T-\sum_j hj\, J_j^{\rightarrow}+\tau_{eff}.V^{\rightarrow}\right)+S_h \quad (10)$$

However, since there is no spices nor viscous heating effects, then the software will solve the equation in the following form:

$$\frac{\partial}{\partial t}\left(\rho\left(e+\frac{V^2}{2}\right)\right)+\nabla.\left(\rho V\left(h+\frac{V^2}{2}\right)\right)=\nabla.\left(k_{eff}\nabla T\right) \quad (11)$$

And given that there is no ventilation inside the room, the heat transfer that is taking place from the gypsum layer in the roof to the indoor air will accrue naturally, and hence natural convection is taking place and that implies the use of Boussinesq density model to capture the flow induced by buoyancy forces, taking into account air density variations due to indoor air temperature changes. As a result of using this model, the density of air is described in the following equation:

$$\rho=\rho_0(1-\beta(T-T_0)) \quad (12)$$

For the cases where the PCM layer is involved, a melting and solidification model is used and the use of this model will change the form of energy equation described above as shown below:

$$\frac{\partial}{\partial t}(\rho H)+\nabla.(\rho V^{\rightarrow}H)=\nabla.(k\nabla T) \quad (13)$$

The liquid fraction is then calculated via the equation below:

$$\alpha=\frac{T-T_s}{T_l-T_s}\ if\ T_s<T<T_l \quad (14)$$

If $T < T_s$, then $\alpha = 0$

If $T > T_l$, then $\alpha = 1$

For the viscous model, laminar model is used considering that the only motion of the indoor air is a result of natural convection, below are the conservation of mass and conservation of momentum respectively:

$$\nabla.V^{\rightarrow}=0 \quad (15)$$

$$\rho(V^{\rightarrow}.\nabla)V^{\rightarrow}=-\nabla p\ +\mu\nabla^2V^{\rightarrow} \quad (16)$$

However, activating the melting and solidification model will add a momentum source term to Eq. (15) that includes a damping effect as shown in Eq. (16).

$$\rho(V^{\rightarrow}.\nabla)V^{\rightarrow}=-\nabla p\ +\mu\nabla^2V^{\rightarrow}-\ \frac{C}{(1-\alpha)^2+\alpha_o}V \quad (17)$$

The added term takes into account the mushy zone in the PCM during phase changes, this zone is where liquid and solid phases coexist. The software treats the mushy zone as a porous medium, and the value of liquid fraction that is calculated based on the enthalpy of PCM represents the porosity of the medium.

An appropriate PCM was chosen according to the range of temperatures of the sand layer in the roof during the day and night times. It should be noted that it's not possible to use the same PCM type for cases (D) & (E) due to the difference in the temperature ranges in the sand layer, using a PCM whose melting temperature range is out of the environment temperature will not activate the PCMs melting and solidification process, hence, it's very crucial to select a PCM type that its melting temperature range within the placed environment temperature. Table 4 shows the properties of the PCMs used in the above cases.

RT38 and RT44 PCMs were used in cases (E) and (D) respectively. As for the boundary conditions, variable heat flux and ambient

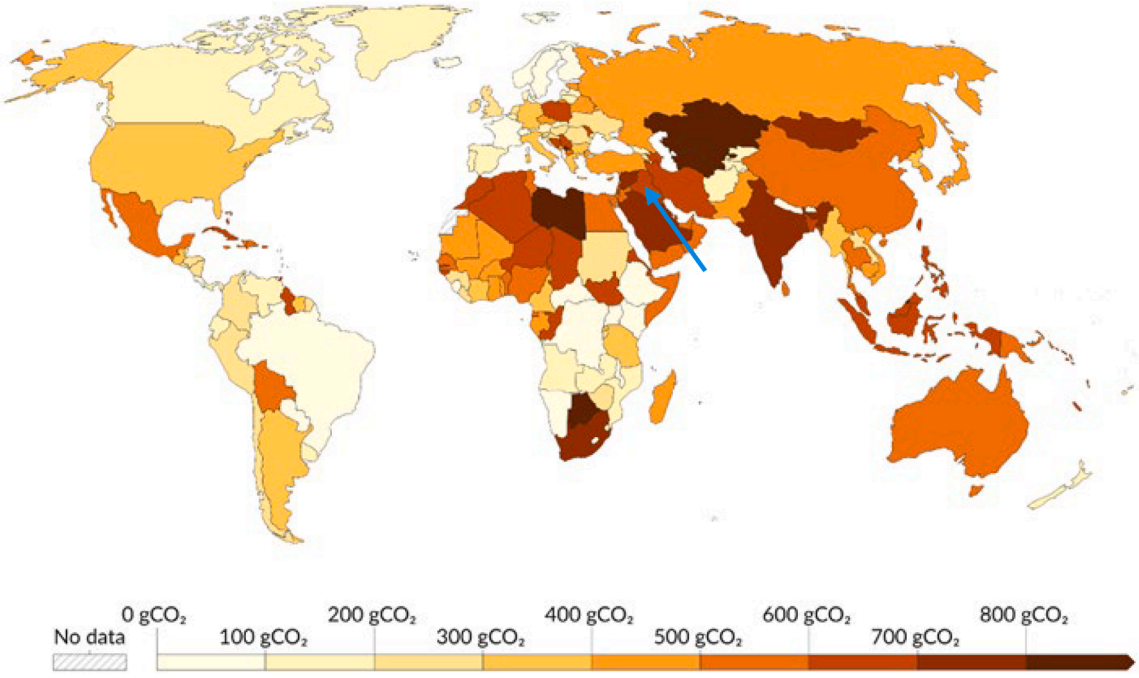

Fig. 4. World map shows the amount of Co2 per kWh [37].

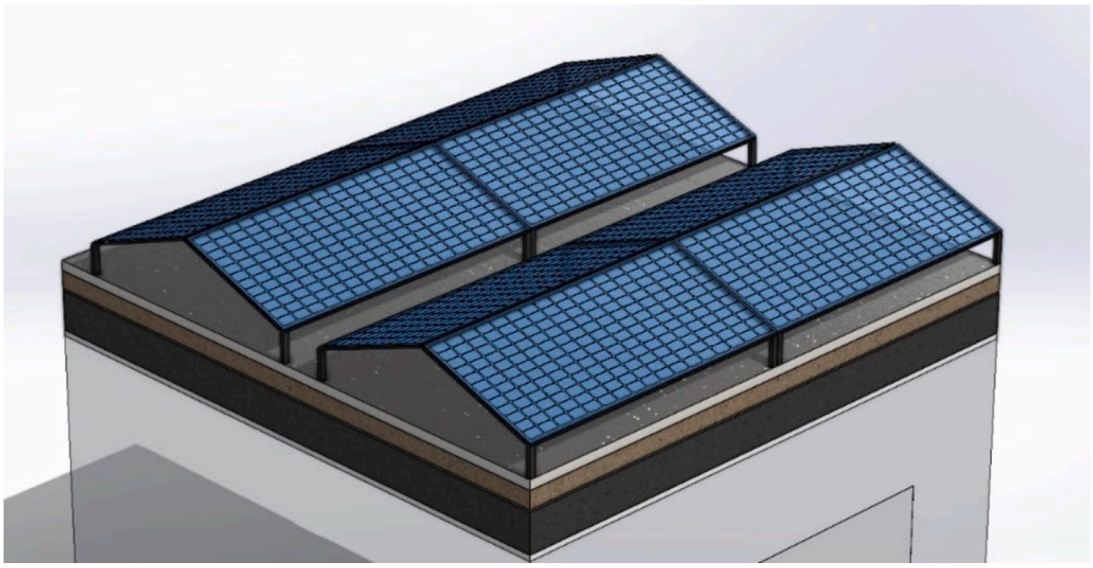

Fig. 5. East-west configuration of solar panels shading the entire roof.

Table 3
GIT results.

Mesh Case	Number Of Cells	Room Indoor Average Temperature Throughout 24 h (k)
1	115,587	309.77
2	210,584	309.87
3	325,523	309.82
4	478,633	309.55
5	562,541	309.85
6	660,842	309.47

temperatures during the 4 days were implied with a constant value of convection heat transfer coefficient. A different set of data was used for the heat flux for the cases being studied.

For cases (A) and (D) the solar radiation was assumed to be fully absorbed by the outer roof layer (cement tiles), and this was implemented as heat generated inside the layer itself with a convection boundary condition on both the cement tiles and the glass window which is assumed to be fully shaded as shown in Fig. 7.

For case (B), in which the roof is assumed to be fully shaded, only convection boundary condition is implemented in the cement tiles surface, along with the glass window.

2.3.3. *Numerical procedure*

No insulation system can be applied without using the right waterproofing approach of the concrete. The critical necessity of cement tiles waterproofing arises from water ingress into concrete due to the formation of pores during the concrete curing phase. Consequently, cement tiles must be protected using various methodologies aimed at reducing

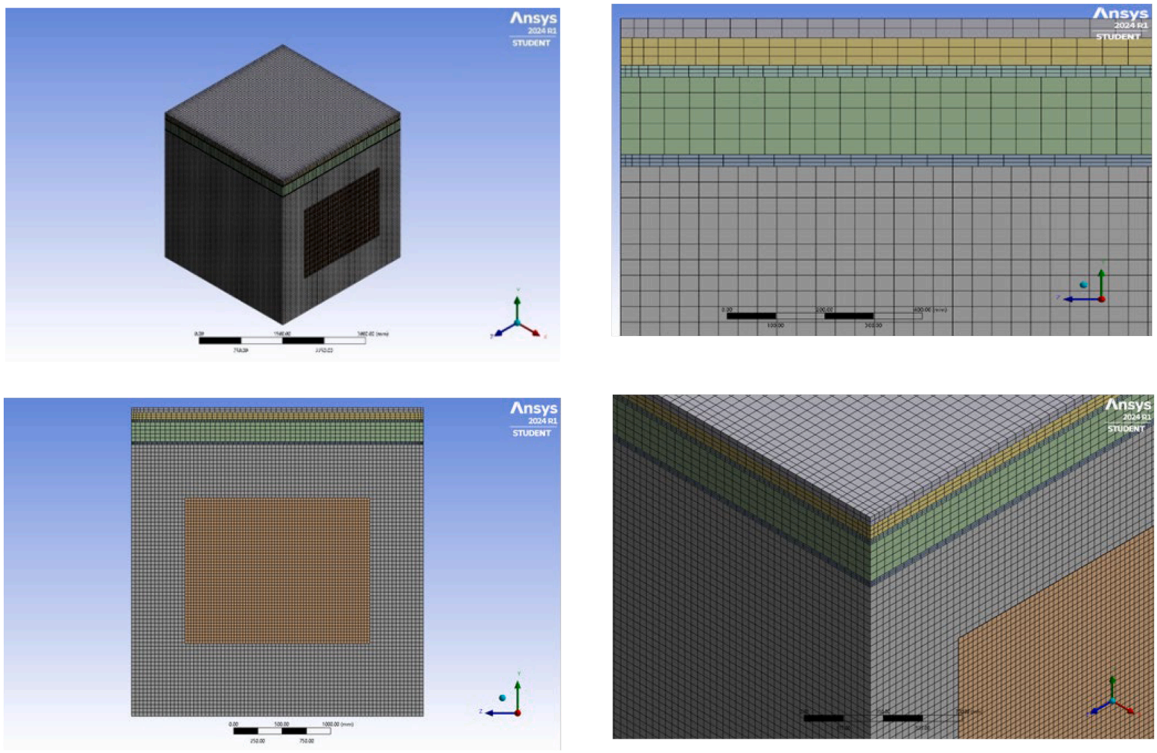

Fig. 6. Multiple views of the generated grid.

Table 4
PCMs properties.

PCM Type	ρ_s (kg/m^3)	ρ_l (kg/m^3)	K(w/m.k)	C_p(j/kg.k)	h_f (kj/kg)	T_s Range(k)	T_l Range (k)
RT38 [39]	880	750	0.2	2000	170	307.16	312.16
RT44 [40]	800	700	0.2	2000	250	314.16	317.16

water penetration, which can cause severe corrosion of reinforcement bars, thereby shortening their service life. In cases (C) and (E) the acrylic paint is painted on the cement tiles surface, which serves as a waterproof and reflective coating with an absorption coefficient of 0.4 [41], i.e., not all the solar radiation is absorbed. The acrylic paint prevents heat from penetrating the room by reflecting the direct radiation away from the room. To ensure an accurate simulation, a time step size of 10 s was selected, resulting in >60,000 data points, with a time step number of 34,560 to obtain a full 4 days (345,600 s). for the pressure-velocity coupling, a SIMPLE solution scheme, acquiring faster convergence in simple flow cases and a second-order upwind for all the governing equations used for more accurate interpolation. The simulation's initial conditions assumed a value of 303.5k for the cement tiles layer and glass, 308.15k for the sand and ferroconcrete, and a value of 296.15k for the gypsum layer and indoor air.

2.4. Validation

To validate the accuracy of our numerical model, we compared our simulation results with experimental data from Al-Yasiri and Szabó [42]. Their study examined the thermal performance of a building envelope integrating PCM and EPS insulation. The numerical methodology used in this validation against the reference room of the experimental study. The room envelope of 1m^3 in their experiment consisted of a 7 cm thick concrete brick wall, a 2 cm thick cement mortar, and a 5 cm thick concrete roof covered with a 0.4 cm isogam layer from the outside and a 0.2 cm gypsum mortar from the inside. We used our numerical model to simulate their exact experimental setup, including boundary conditions and material properties. Comparing our simulation results with their experimental data, we found that our model accurately predicted the indoor temperature of the test room, with an average error of 14.74 % and a maximum error of 22.31 %. This validation confirms that our numerical model is reliable for predicting the thermal performance of building envelopes. It can be used to optimize envelope designs for various climates and building types. Fig. 8 shows that the numerical approach follows the same experimental trend of average indoor reference room temperature. The observed discrepancies between experimental and numerical results, can be attributed to inherent numerical assumptions such as constant material properties and convection heat transfer coefficients, as well as potential experimental measurement errors. These factors, while acknowledged, do not undermine the overall confirmation of our methodology's effectiveness.

Therefore, this validation not only confirms the simulation results but, more importantly, establishes the validity of our numerical methodology for predicting the thermal performance of PCM-integrated building envelopes. This validated approach can now be confidently applied to optimize envelope designs across diverse climates and building types.

3. Results

The current study exposes a holistic simulation of thermal management strategies for evaluating several techniques' effectiveness in reducing heat flow into the buildings for later energy consumption reduction in the Middle Eastern region, specifically in Iraq, from August 16–19. The above month is generally characterized by desert ambient

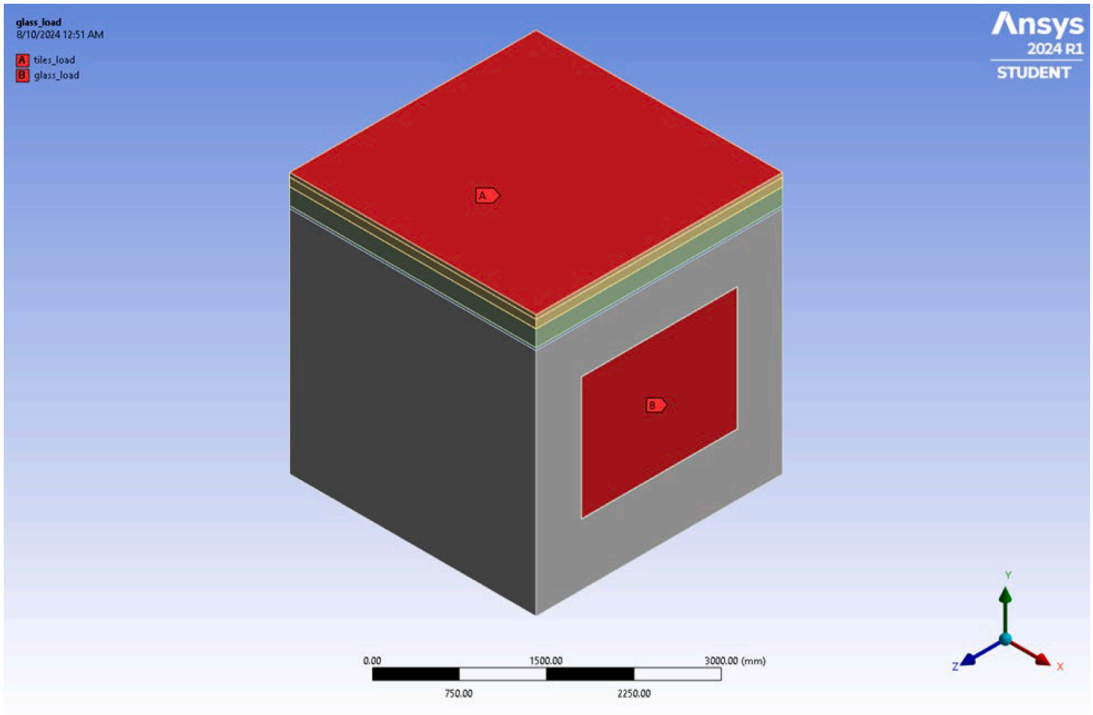

Fig. 7. Named selections of the boundary conditions.

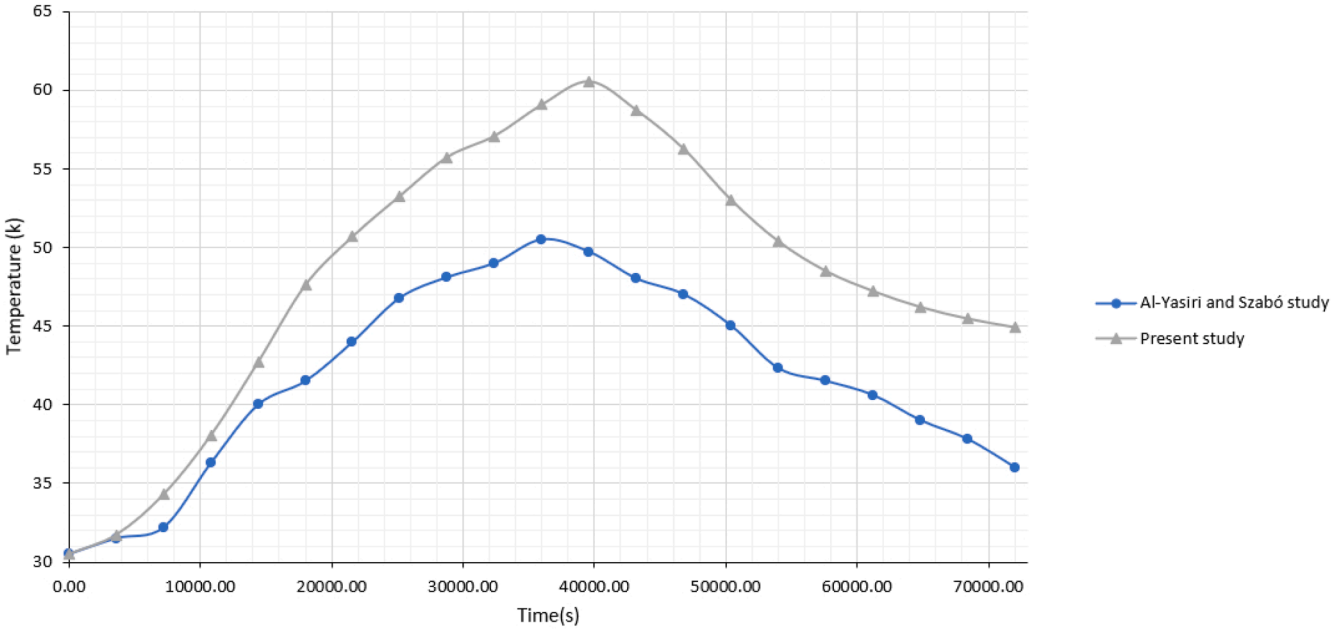

Fig. 8. Average indoor room temperature for the present study against Al-Yasiri and Szabó.

Table 5
Thermal performance and emissions across simulated cases.

Case	Peak Temperature (K)	Minimum Temperature (K)	ΔT (K)	Standard Deviation (K)	Heat Flow Reduction (%)	CO_2 Emissions (kg/4 days)
A	320.45	300.12	20.33	6.25	0	9.151
B	309.96	298.85	11.11	3.68	92.69	0.671
C	314.16	299.47	14.69	4.25	56.70	5.767
D	315.52	300.09	15.43	4.78	73.65	3.797
E	313.66	299.85	13.81	4.11	84.12	2.114

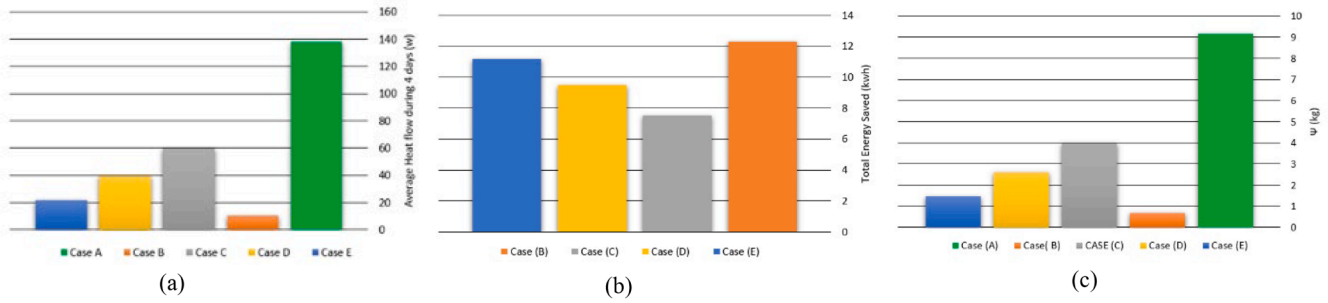

Fig. 9. a) Average value of Heat flow through the room; b) Total amount of energy saved for the 4 cases; c) Amount of Co2 consumed for each case. Measurement was conducted for 4 days.

air conditions, whereby daily temperatures can exceed 45 °C and remain at night temperatures of over 30 °C, especially in July and August. The outdoor temperature and solar heat flux data were obtained from Metronome software, which has Worldwide irradiation data under Typical years and historical time series. The study outlines five cases as shown in Table 1. The strategies' effectiveness was evaluated by heat flow reduction, indoor temperature stabilization, and minimized demand for cooling energy as summarized in Table 5 summary of all cases.

The findings revealed that the lowest heat flow reduction was achieved under Case A with highest range of instability of indoor peak temperature around 320.45 K, a fluctuation range of 20.33 K, and a standard deviation of 6.25 K. In contrast, Case B using Full roof shading with east-west PV panels achieved **92.69 %**, the highest among all cases. Peak indoor temperatures dropped to **309.96 K,** a fluctuation range of 11.11 K, and a standard deviation of 3.68 K as given in Fig. 9. They effectively block direct solar radiation so that roof surface temperatures are reduced significantly. This method will be more successful in regions with high solar radiation characteristics since it then directly reduces the heat gained at peak hours. in (Case C) our study concentrates on the Reflective coatings utilization to reflect solar radiation. The paint technique showed moderate improvements with a maximum heat flow reduction of 56.70 % and a peak temperature of 314.16 K with a fluctuation range of about 14.69 K and a standard deviation of 4.25 K, indicating moderate stabilization. The reflective paint absorbs solar radiation and reflects a substantial portion of it, thereby inhibiting its penetration into space. Although reflective coatings improve conditions moderately, they are very poor at peak desert conditions due to pre-reflection heat absorption. PCM's thermal storage capabilities buffered temperature swings by absorbing heat during the daytime and then releasing it at nighttime. Therefore, PCM integration moderates daytime

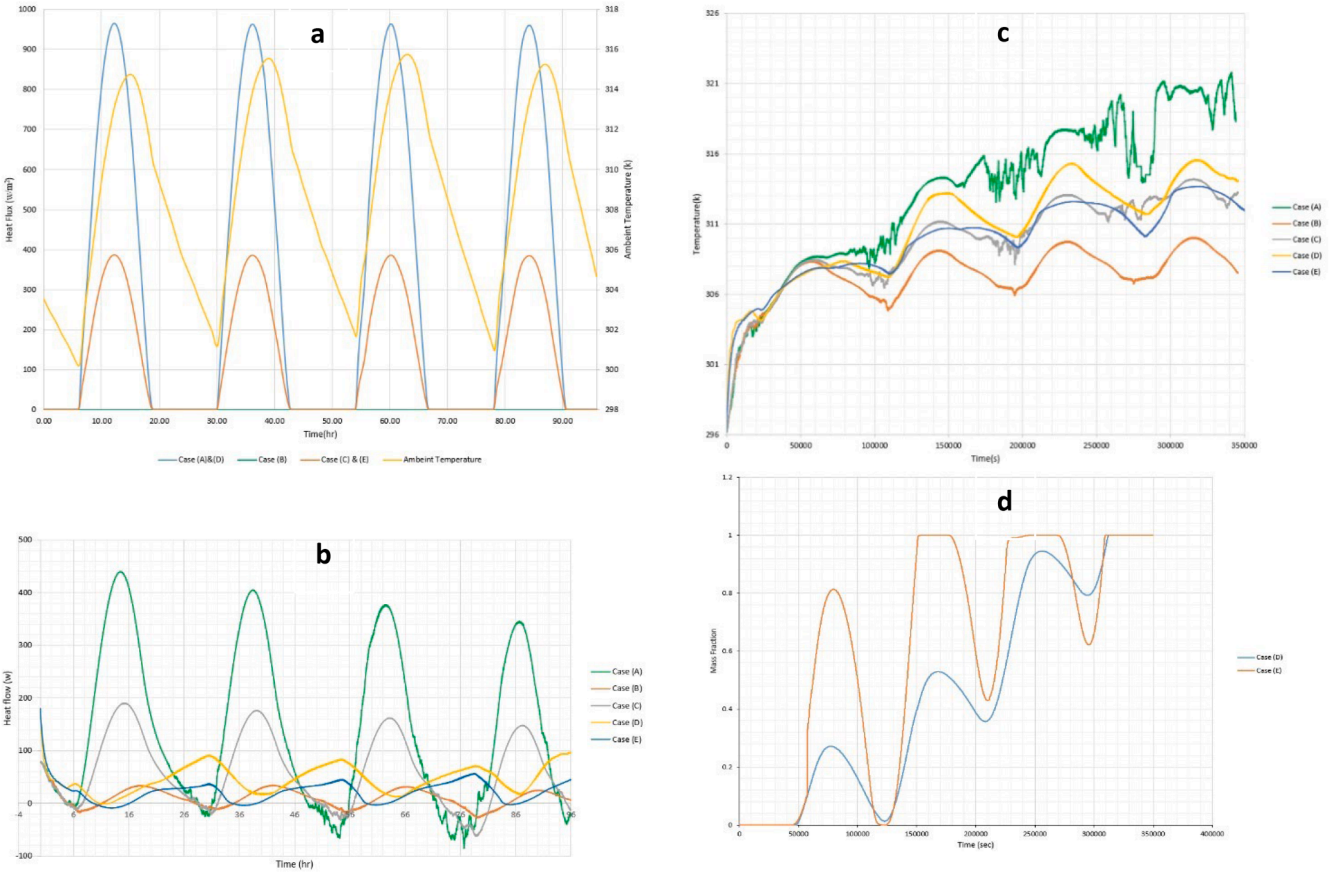

Fig. 10. a) Heat flux trends and ambient temperature, b). Heat flows through the room for all the cases for 4 days; c) Average indoor room temperatures; d) Average Mass fraction of PCM layer.

temperatures and increases nighttime degrees slightly due to the discharge effect.

The heat flow was reduced by 73.65 % in Case D, which incorporates PCM. The peak temperature was 315.52 K, the ΔT was 15.43 K, and the standard deviation was 4.78 K. Case D's PCM integration effectively dampens temperature fluctuations, and thermal regulation has other advantages, such as storing heat during the day and releasing it at night to maintain precisely cycling indoor temperatures. With a peak temperature of 313.66 k, a temperature gradient (ΔT) of 13.81 k, and a standard deviation of 4.11 k, Case E was able to reduce heat flow by 84.12 %. Over the course of four days, the integration of PCM in case E considerably stabilized temperatures, revealing glasses with decreased interior temperature variation (ΔT) at standard deviation. Case (E) was more advantageous than Case (D) because of the synergies that resulted from using reflective paint and PCM, which enhanced heat reflection and storage simultaneously. If we compare the melting and solidification mass fractions of the PCM layer in cases (D) and (E) (Fig. 10d)), we can see that Case (E) experiences more activation than Case (D) over the course of the four days. This is likely due to the fact that Case (E) makes use of PCM with a smaller melting temperature area than Case (D), and because applying acrylic paint to the outside of the roof decreases the heat flow into the room.

From these cases, it is evident that Case (E) has higher thermal efficiency because when the reflective coating is combined with the PCM, the energy savings are maximum and consequently benefit by reduced cooling energy demand towards more consistent indoor temperature regulation and enhanced indoor thermal comfort. The temperature variations, on the one hand, bring energy efficiency results, to such a case, for instance, Case E, where reflective paint led to PCM activation since it reduced initial heat flow. In that case, combined strategies induced maximum energy efficiency because in just four days CO_2 emissions were reduced to 2.114 kg, as against 9.151 kg in Case A (see Fig. 9c). However, Case (B) recorded the lowest CO2 consumption over four days, and it has 0.671 kg. On the other hand, reflective coating alone emitted 5.767 kg (Case C), while PCM-integrated only produced 3.797 kg (Case D). These results show how lowered temperature variability directly affects energy consumption and greenhouse gas emissions. In each case, the highest air temperature indoors is noted to be closer to the gypsum layer directly involved by convection heat transfer between the gyps and the air as is shown in Fig. 11(a–d). Contours show that Case B is observed as cooler than Case A within the peak solar hours. Furthermore, Case (E) exhibits the least variable temperature regime.

Hence, hot air accumulates at the top causing even hotter areas around that as indicated in Fig. 12(a–d). The integration of passive

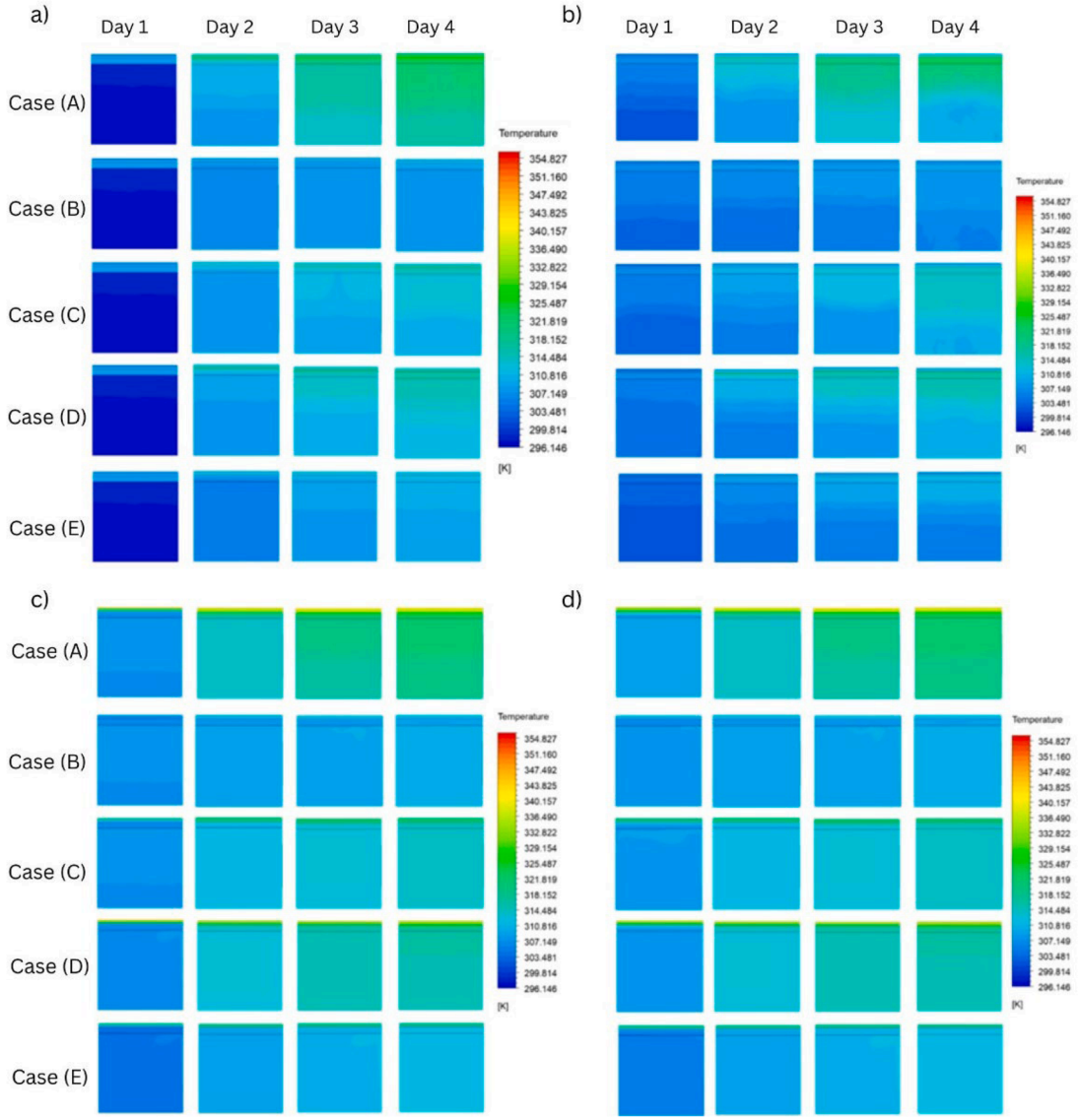

Fig. 11. Mid-plane room temperature counters of all cases (A-E) at a) 12:00 AM, b) 6:00 AM, c) 12:00 PM, d) 6:00 PM for 4 days.

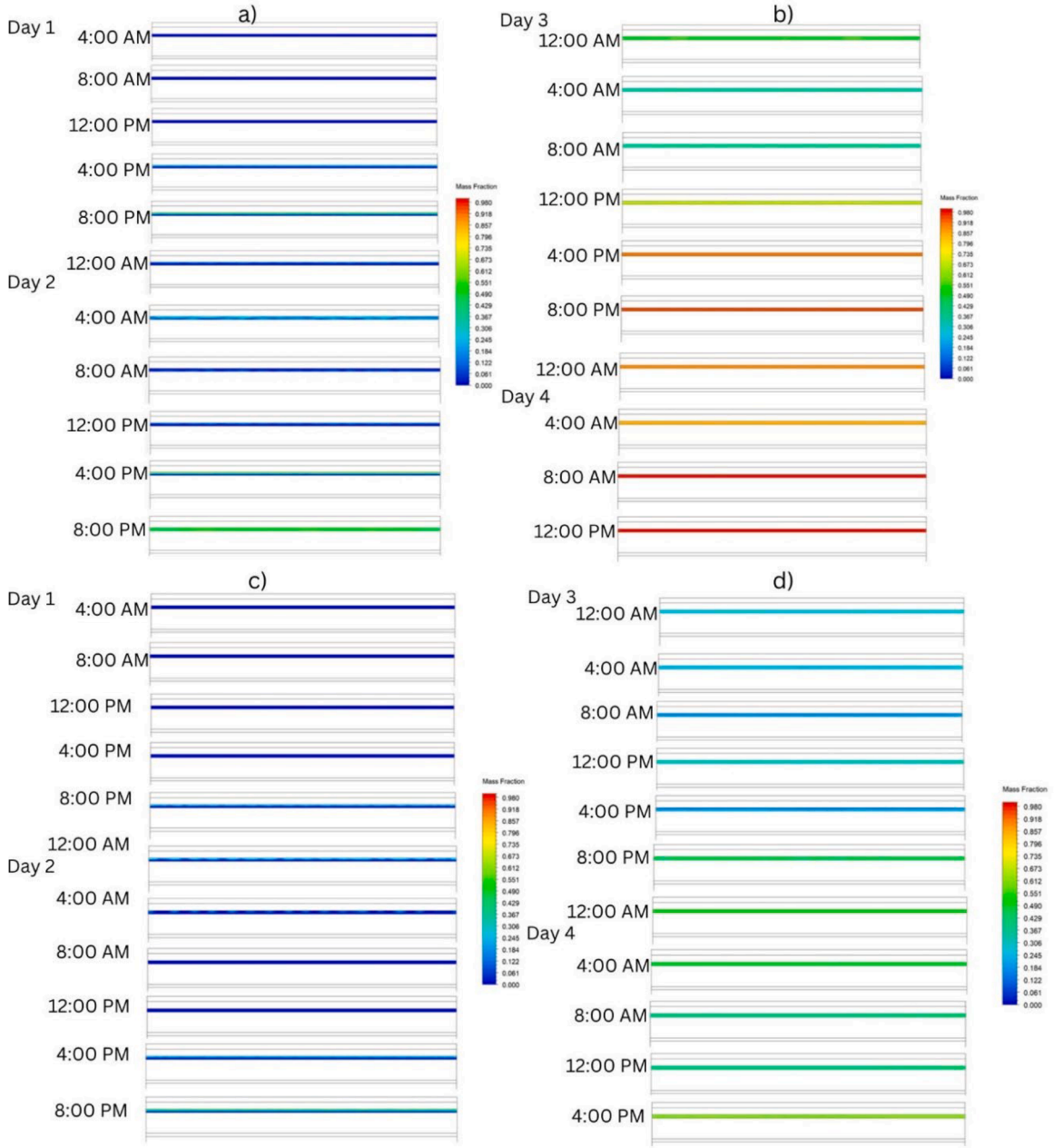

Fig. 12. PCM Mass fraction for case (D) during days a) 1, 2; b) 3, 4 every 4 h, and case (E) during days c) 1, 2; d) 3 and 4 every 4 h.

techniques such as Cases (D) and (E) has succeeded in prolonging the point of indoor temperature peak. The analysis of the energy saving and indoor temperature reduction in association with the combination of PCM with reflective coating, Case (E), indicated significant savings and temperature reductions as a result of applying reflective paint together with PCM. Certainly, such data will provide building energy efficiency improvements in the eastern Mediterranean and Middle Eastern countries. Such strategies may also help in reducing energy consumption for conditioning, and greenhouse gas emissions, and improving indoor thermal comfort towards the sustainability of buildings in hot desert climates.

4. Discussion

The findings of this study demonstrate the effectiveness of integrating phase-change materials (PCMs), reflective coatings, and solar shading in improving the energy efficiency of buildings in hot climates. The results highlight the potential of these passive cooling strategies to reduce heat flow, stabilize indoor temperatures, and minimize CO_2 emissions. Case (D) aligns with Dardouri et al. evaluated PCM-insulation combinations in Tunisian climates, demonstrating energy savings of up to 76.46 % with a double PCM layer in double-wall structures as they resulted in very stable indoor temperatures and significant energy savings [22]. however, The combination of PCM with reflective coatings (Case E) achieved higher heat flow reduction of 84.12 %, indicating a 7.66 % increase in energy saving compared with Dardouri et al. More on Case (D),Al-Yasiri and Szabó [42] researched how to integrate PCM with EPS insulation to form a building envelope with improved performance given harsh summer conditions, which is analogous to Case (D) in our study that in fact, demonstrated benefits from PCM integration for improving their results. They reported improvements in thermals inertia with an indoor temperature reduction (MITR) of 143 %. There was also a time lag increase of 177.2 % when compared with PCM-only configurations, giving importance to optimized EPS thickness (1–2 cm). Liu

et al. [43] optimized PCM parameters for lightweight building walls, which reduced the peak heat flux up to 66.52 %, making it more effective than Case (C), and less effective compared with Cases (B),(D), and (E). While our results (Case D: 73.65 %) bridge this gap by tailoring PCM melting points to Iraq's climate. Similarly, Yu et al. [24] published CFD simulations to perform analysis over PCM roofs across the climate zones with decrement factor reductions of >85 %. While this study provides valuable insights, it has some limitations that should be addressed in future research. The simulations assumed no ventilation and no indoor heat sources, which may not reflect real-world conditions. Future studies should incorporate these factors to provide a more accurate assessment of thermal performance. The cost of implementing PCM, reflective coatings, and solar shading was not considered in this study. Future work should evaluate the economic feasibility of these strategies, including installation and maintenance costs.

5. Conclusions

This study validates experimental data to simulation results, thus rendering the outcomes more credible than models built just with numeric simulations. The integrated system of phase change materials (PCM), reflective acrylic coatings, and solar panel roof shading all show well-increased improvement in thermal performance and energy efficiency for residential buildings in hot climates. The experimental validation of (CFD) simulations using real weather data in ANSYS Fluent has demonstrated temperature reductions as well as energy savings for all cases evaluated. Such cases include roof shading with solar panels (Case B), which led to the maximum reduction in indoor temperature, reaching a peak of 309.96 K, compared with 320.45 K for the baseline (Case A), thus having a difference of 10.49 K. Using reflective paint in conjunction with PCM (Case E), the peak indoor temperature was reduced down to 313.66 K, leading to a 6.79 K decrease, yet also the most stable temperature profile (ΔT = 13.81 K, standard deviation = 4.11 K). This is the first study to assess many passive cooling techniques and introduces some new performance metrics for thermal performance and the impact on the environment, such as temperature fluctuation ranges (ΔT) and CO_2 emissions by case. Thus, it has been proved that indoor thermal comfort was improved by combining heat reflection and thermal storage, which reduces cooling demands through the integration of reflective coatings with PCM. These findings provide a premise for sustainable buildings.

CRediT authorship contribution statement

Mohammed ALamin Talib Mahdi: Writing – review & editing, Writing – original draft, Visualization, Software, Methodology, Investigation, Data curation, Conceptualization. **Mousa Nader:** Writing – review & editing, Writing – original draft, Resources, Investigation, Data curation, Conceptualization. **Humam Yagdan:** Writing – review & editing, Writing – original draft, Resources. **Sajjad Tariq:** Writing – review & editing, Writing – original draft, Resources. **Amar S. Abdul-Zahra:** Writing – review & editing, Supervision, Methodology, Conceptualization. **Hussaen A.H. Kahachi:** Writing – review & editing, Visualization, Supervision, Project administration.

Declaration of competing interest

The authors declare that they have no known competing financial interests or personal relationships that could have appeared to influence the work reported in this paper.

Declaration of generative AI and AI-assisted technology in the writing process

During the preparation of this work, the authors used perplexity, Litmaps, and scispace in order to enhance the research by ensuring accuracy, tracking scientific literature trends, and streamlining the understanding and presentation of complex concepts. After using those tools, the authors reviewed and edited the content as needed and takes full responsibility for the content of the publication.

Acknowledgments

The authors acknowledge the support of Reach Sci organization for supporting with lectures and mentoring. And Hadeel Jamel for providing consultants and support.

Data availability

Data will be made available on request.

References

[1] EDGAR - The Emissions Database for Global Atmospheric Research, (n.d.),(2023) https://edgar.jrc.ec.europa.eu/report_2023 (accessed December 27, 2024).
[2] United Nations Environment Programme, Emissions Gap Report 2023: Broken Record – Temperatures hit new highs, yet world fails to cut emissions (again), United Nations Environment Programme, 2023. https://doi.org/10.59117/20.500.11822/43922.
[3] M. Venturelli, R. Saponelli, M. Milani, L. Montorsi, Combined numerical approach for the evaluation of the energy efficiency and economic investment of building external insulation technologies, Energy Nexus 10 (2023) 100198, https://doi.org/10.1016/j.nexus.2023.100198.
[4] Committee on Development of a, Framework for Evaluating Global Greenhouse Gas Emissions Information for Decision Making, Board on Atmospheric Sciences and Climate, Division on Earth and Life Studies, National Academies of Sciences, Engineering, and Medicine, Greenhouse Gas Emissions Information For Decision Making: A Framework Going Forward, National Academies Press, Washington, D. C., 2022, https://doi.org/10.17226/26641.
[5] G. Zittis, M. Almazroui, P. Alpert, P. Ciais, W. Cramer, Y. Dahdal, M. Fnais, D. Francis, P. Hadjinicolaou, F. Howari, A. Jrrar, D.G. Kaskaoutis, M. Kulmala, G. Lazoglou, N. Mihalopoulos, X. Lin, Y. Rudich, J. Sciare, G. Stenchikov, E. Xoplaki, J. Lelieveld, Climate change and weather extremes in the eastern mediterranean and middle east, Rev. Geophys. 60 (2022), https://doi.org/10.1029/2021RG000762 e2021RG000762.
[6] U.S. energy consumption by source and sector, 2023. https://www.eia.gov/totalenergy/data/monthly/,2023 (accessed 24 September 2024).
[7] M. Röck, M.R.M. Saade, M. Balouktsi, F.N. Rasmussen, H. Birgisdottir, R. Frischknecht, G. Habert, T. Lützkendorf, A. Passer, Embodied GHG emissions of buildings – The hidden challenge for effective climate change mitigation, Appl. Energy 258 (2020) 114107, https://doi.org/10.1016/j.apenergy.2019.114107.
[8] J. Torres-Quezada, H. Coch, A. Isalguè, J. López, The roof impact on the heat balance of low height buildings at low latitudes, 2018.
[9] M.F. Idan, Reducing the cost of energy used for adaptation by using different exterior wall covering materials in Iraq, IJAAS 11 (2022) 177, https://doi.org/10.11591/ijaas.v11.i3.pp177-186.
[10] R. Kaya, S. Caglayan, Potential Benefits of Thermal Insulation in Public Buildings: Case of a University Building, Buildings 13 (2023) 2586. https://doi.org/10.3390/buildings13102586.
[11] A.M. Raimundo, A.M. Sousa, A.V.M. Oliveira, Assessment of energy, environmental and economic costs of buildings' Thermal insulation–Influence of type of use and climate, Buildings 13 (2023) 279, https://doi.org/10.3390/buildings13020279.
[12] Hamza Shaikh, R.A. Memon, S. Qureshi, A. Shaikh, S.A. Noonari, The impact of the wall insulation material and variable refrigerant flow system on building energy consumption and cost, JMES (2023) 9383–9394, https://doi.org/10.15282/jmes.17.1.2023.8.0742.
[13] A. Hussein, A. Saleh, H. Ahmed, Numerical study of the effect of thermal insulation and window-to-wall ratio on reducing the thermal loads of the residential sector in Iraq, ETJ 0 (2023) 1–12, https://doi.org/10.30684/etj.2023.143408.1584.
[14] A. Siciliano, X. Zhao, R. Fedderwitz, K. Ramakrishnan, J. Dai, A. Gong, J. Zhu, J. Kośny, L. Hu, Sustainable wood-waste-based thermal insulation foam for building energy efficiency, Buildings 13 (2023) 840, https://doi.org/10.3390/buildings13040840.
[15] A. Mahmood, H. Qatta, N. Hussein, Effect of using local insulation materials on the indoor temperature of residential buildings at Iraq, ETJ 37 (2019) 37–45, https://doi.org/10.30684/etj.37.2A.1.
[16] J. Bravo, T. Venegas, E. Correa, A. Álamos, F. Sepúlveda, D. Vasco, C. Barreneche, Experimental and computational study of the implementation of mPCM-modified gypsum boards in a test enclosure, Buildings 10 (2020) 15, https://doi.org/10.3390/buildings10010015.
[17] U. Bordoloi, B. Das, Enhancing thermal comfort in buildings through the integration of phase change material on the building envelope: a simulation study, IOP Conf. Ser.: Earth Environ. Sci. 1372 (2024) 012089, https://doi.org/10.1088/1755-1315/1372/1/012089.
[18] S. Cesari, E. Baccega, G. Emmi, M. Bottarelli, Enhancement of a radiant floor with a checkerboard pattern of two PCMs for heating and cooling: results of a real-scale

monitoring campaign, Appl. Therm. Eng. 246 (2024) 122887, https://doi.org/10.1016/j.applthermaleng.2024.122887.
[19] F. Rebelo, A. Figueiredo, R. Vicente, R.M.S.F. Almeida, H. Paiva, V.M. Ferreira, Development of innovative mortars incorporating phase change materials and by-products for high performance radiant floor systems, Constr. Build. Mater. 420 (2024) 135488, https://doi.org/10.1016/j.conbuildmat.2024.135488.
[20] M. Izadi, S.F. Taghavi, S.H. Neshat Safavi, F. Afsharpanah, W. Yaïci, Thermal management of shelter building walls by PCM macro-encapsulation in commercial hollow bricks, Case Studies in Thermal Engineering 47 (2023) 103081, https://doi.org/10.1016/j.csite.2023.103081.
[21] J. Skovajsa, P. Drabek, S. Sehnalek, M. Zalesak, Design and experimental evaluation of phase change material based cooling ceiling system, Appl. Therm. Eng. 205 (2022) 118011, https://doi.org/10.1016/j.applthermaleng.2021.118011.
[22] S. Dardouri, S. Mankai, M.M. Almoneef, M. Mbarek, J. Sghaier, Energy performance based optimization of building envelope containing PCM combined with insulation considering various configurations, Energy Reports 10 (2023) 895–909, https://doi.org/10.1016/j.egyr.2023.07.050.
[23] D.K. Bhamare, M.K. Rathod, J. Banerjee, M. Arıcı, Investigation of the effect of air layer thickness on the thermal performance of the PCM Integrated roof, Buildings 13 (2023) 488, https://doi.org/10.3390/buildings13020488.
[24] J. Yu, K. Leng, F. Wang, H. Ye, Y. Luo, Simulation study on dynamic thermal performance of a new ventilated roof with form-stable PCM in Southern China, Sustainability 12 (2020) 9315, https://doi.org/10.3390/su12229315.
[25] H. Abbas, J. Jalil, S. Ahmed, Experimental investigation of the optimal location of PCM capsules in a hollow brick wall, ETJ 39 (2021) 846–858, https://doi.org/10.30684/etj.v39i5A.1980.
[26] C. Mano, A. Thongtha, Enhanced thermal performance of roofing materials by integrating phase change materials to reduce energy consumption in buildings, J. Renew. Mater. 9 (2021) 495–506, https://doi.org/10.32604/jrm.2021.013201.
[27] P. Mokhberi, P. Mokhberi, M. Izadi, M. Bagheri Nesaii, W. Yaici, F. Minelli, Thermal regulation enhancement in multi-story office buildings: integrating phase change materials into inter-floor void formers, Case Studies Thermal Eng. 60 (2024) 104792, https://doi.org/10.1016/j.csite.2024.104792.
[28] A. Albatayneh, R. Albadaineh, A. Juaidi, R. Abdallah, M.D.G. Montoya, F. Manzano-Agugliaro, Rooftop photovoltaic system as a shading device for uninsulated buildings, Energy Reports 8 (2022) 4223–4232, https://doi.org/10.1016/j.egyr.2022.03.082.
[29] M. Zubair, A. Bilal Awan, A. Al-Ahmadi, A.G. Abo-Khalil, NPC based design optimization for a net zero office building in hot climates with PV panels as shading device, Energies 11 (2018) 1391, https://doi.org/10.3390/en11061391.
[30] H. Alasadi, J.-K. Choi, R.B. Mulford, Influence of photovoltaic shading on rooftop heat transfer, building energy loads, and photovoltaic power output, J. Sol. Energy Eng. 144 (2022) 061011, https://doi.org/10.1115/1.4054710.
[31] Y. Cai, Y. Huang, Z. Shu, Z. Liu, H. Zhong, F. Zhao, Investigation of double-PCM based PV composite wall for power-generation and building insulation: thermal characteristics and energy consumption prediction, Energy Built Environ. (2024), https://doi.org/10.1016/j.enbenv.2024.08.002. S2666123324000795.
[32] R. Vanaga, J. Narbuts, Z. Zundāns, J. Gušča, Systematic literature review of software tools for modeling heat transfer in phase change materials for building applications, IOP Conf. Ser.: Earth Environ. Sci. 1372 (2024) 012017, https://doi.org/10.1088/1755-1315/1372/1/012017.
[33] Iraqi Ministry of Construction and Housing, General Authority for Buildings, Ministry of Planning and the Central Organization For Standardization and Quality Control, Iraqi Cooling Code, first ed., Baghdad, 2014.
[34] Heat Transfer, Tenth Edition.pdf, (2002).
[35] M.E. Afshan, A.G. Lucas, Technology in Design of Heat Exchangers for Thermal Energy Storage, Phase Change Mater. (2022).
[36] M. Salihi, M. El Fiti, Y. Harmen, Y. Chhiti, A. Chebak, F.E. M'Hamdi Alaoui, M. Achak, F. Bentiss, C. Jama, Evaluation of global energy performance of building walls integrating PCM: numerical study in semi-arid climate in Morocco, Case Studies Constr. Mater. 16 (2022) e00979, https://doi.org/10.1016/j.cscm.2022.e00979.
[37] S. Busto, M. Dumbser, A new thermodynamically compatible finite volume scheme for magnetohydrodynamics, SIAM J. Numer. Anal. 61 (2023) 343–364, https://doi.org/10.1137/22M147815X.
[38] Manual User. "ANSYS FLUENT 22.0" Theory guide, 2022.
[39] Rubitherm phase change material, 2024. https://www.rubitherm.eu/en/productcategory/organische-pcm-rt.
[40] Rubitherm phase change material, 2024. https://www.rubitherm.eu/en/productcategory/organische-pcm-rt.
[41] A. Azemati, S.S. Rahimian Koloor, H. Khorasanizadeh, G. Sheikhzadeh, B. S. Hadavand, M. Eldessouki, Thermal evaluation of a room coated by thin urethane nanocomposite layer coating for energy-saving efficiency in building applications, Case Studies Thermal Eng. 43 (2023) 102688, https://doi.org/10.1016/j.csite.2022.102688.
[42] Q. Al-Yasiri, M. Szabó, Building envelope-combined phase change material and thermal insulation for energy-effective buildings during harsh summer: simulation-based analysis, Energy Sustain. Dev. 72 (2023) 326–339, https://doi.org/10.1016/j.esd.2023.01.003.
[43] Z. Liu, J. Hou, X. Meng, B.J. Dewancker, A numerical study on the effect of phase-change material (PCM) parameters on the thermal performance of lightweight building walls, Case Studies Construct. Mater. 15 (2021) e00758, https://doi.org/10.1016/j.cscm.2021.e00758.